THE JOURNAL OF PHYSICAL CHEMISTRY Letters

LETTER

pubs.acs.org/JPCL

Effects of Coadsorbed Oxygen on the Infrared Driven Decomposition of N_2O on Isolated Rh_5^+ Clusters

Alexander C. Hermes,[†] Suzanne M. Hamilton,[†] W. Scott Hopkins,[†,§] Dan J. Harding,[‡] Christian Kerpal,[‡] Gerard Meijer,[‡] André Fielicke,[*,‡] and Stuart R. Mackenzie[*,†]

[†]Department of Chemistry, University of Oxford, South Parks Road, Oxford, OX1 3QZ, U.K.

[‡]Fritz-Haber-Institut der Max-Planck-Gesellschaft, Faradayweg 4-6, Berlin, D-14195, Germany

Supporting Information

ABSTRACT: The thermally induced decomposition of nitrous oxide on isolated Rh_5^+ and Rh_5O^+ clusters has been investigated using mid-infrared multiple photon dissociation spectroscopy. The presence of a single coadsorbed oxygen atom is observed to have a profound effect on the cluster surface processes that ensue following infrared heating of the cluster. Exciting the infrared active N_2O bending transition in $Rh_5N_2O^+$ results predominantly (≥85%) in molecular desorption of the N_2O moiety, while the same excitation in $Rh_5ON_2O^+$ leads instead to N_2O dissociation on the cluster surface producing $Rh_5O_2^+$ (≥85%). Calculations of the reaction pathway using density functional theory indicate that the change in branching ratio arises from a 0.4 eV greater binding energy of N_2O to Rh_5O^+ compared with Rh_5^+, taking the desorption threshold above the reaction barrier for the surface reaction channel whose energy is unchanged.

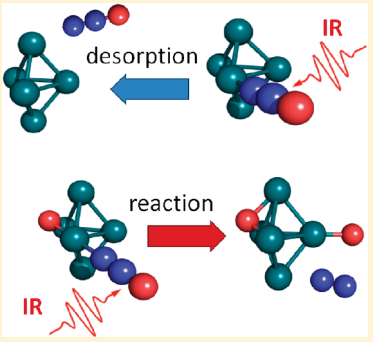

SECTION: Dynamics, Clusters, Excited States

It is well established that in the nanocluster regime of less than 20 or so atoms, metal particles exhibit unique size-dependent physical and chemical properties. Indeed, developing a better understanding of the evolution of the geometric and electronic structure of isolated clusters with size remains a central aim of cluster science. Nowhere is this more challenging than for transition metal clusters for which, despite their relevance to practical catalysts, a coherent picture is yet to emerge.

Real heterogeneous catalysts often involve reaction at small imperfections or defect sites, rather than at bulk crystalline surfaces.[1] The appealing idea that small transition metal clusters, with no long-range order at all, may represent experimentally and computationally tractable model systems for such defects[2,3] has sparked intense interest in isolated transition metal clusters. One environmentally important process, the reduction of nitrogen oxides on rhodium clusters, has been the subject of a number of recent studies by (part of) this group and others.[2−7]

It is well established that atomic and molecular adsorbates can dramatically affect the reactivity of a catalytic metal surface, promoting or inhibiting ('poisoning') various processes. Such effects can arise due to the geometry of adsorption (blocking) or through electronic effects, and they form an important part of understanding the activity of a catalyst.[8] In turn, cooperative and competitive binding effects, in which the adsorption of one species affects the binding of another, can play similarly profound roles in governing the reactivity of small isolated metal clusters such as gold clusters.[9−12] This paper describes just such an effect involving the oxygen enhanced binding of nitrous oxide on small rhodium clusters.

In the gas phase, infrared multiple photon dissociation (IR-MPD) spectroscopy has become the technique of choice for measuring the vibrational spectra of transition metal clusters.[13−16] In this technique the absorption of IR photons is detected by the loss of a weakly bound species—a chromophore or an inert tag—using mass spectrometric techniques. The high fluence and wide wavelength tuneability of modern laser sources combined with the inherent sensitivity of mass spectrometry permits the measurement of size-specific vibrational spectra of metal clusters in low-density molecular beams.

Very recently, we have shown that resonant IR absorption may also be used to trigger chemical reactivity on the surface of isolated metal clusters.[17,18] In a cluster analogue of a temperature programmed reaction, $Rh_nN_2O^+$ cluster complexes may be excited via the nitrous oxide vibrational modes, resulting in heating of the complexes and the subsequent dissociation of the molecularly adsorbed N_2O moiety. The net result is the production of the oxide cluster, Rh_nO^+, and molecular nitrogen which desorbs. For most cluster sizes, this reaction occurs as a significant minor channel along with simple N_2O desorption. Reflecting the thermal nature of the chemistry involved, the IR-induced reaction was observed for each of the cluster sizes n = 4, 6−8 with comparable efficiency, irrespective of the vibrational mode pumped. Uniquely in the cluster size range studied, $Rh_5N_2O^+$ exhibits markedly reduced surface reactivity, with N_2O desorption dominating.

Received: September 23, 2011
Accepted: November 16, 2011
Published: November 16, 2011

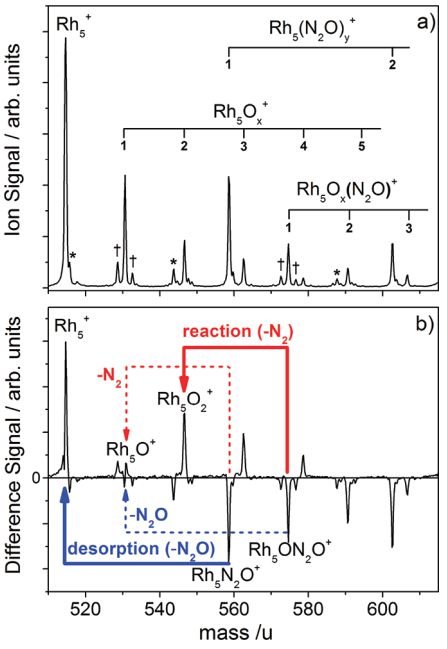

Figure 1. (a) Mass spectrum in the region of the Rh_5^+ clusters recorded in the absence of infrared irradiation. (*) Rh_4^+-based species and (†) minor background Rh_5R^+ species (R = N, H_2O, *etc.*) in the beam. (b) Difference mass spectrum (FELIX on−FELIX off). The 'on' mass spectrum is the sum of the mass spectra collected with FELIX tuned across the fwhm of the N_2O bend/Rh_5−O spectral feature (see Figure 2). On the basis of panel b as well as data from IR-MPD spectra, we can conclude that N_2O desorption is the dominant IR-induced process observed for $Rh_5N_2O^+$ with little evidence of the reactive (N_2 loss) channel. The opposite is true for $Rh_5ON_2O^+$. See text for details.

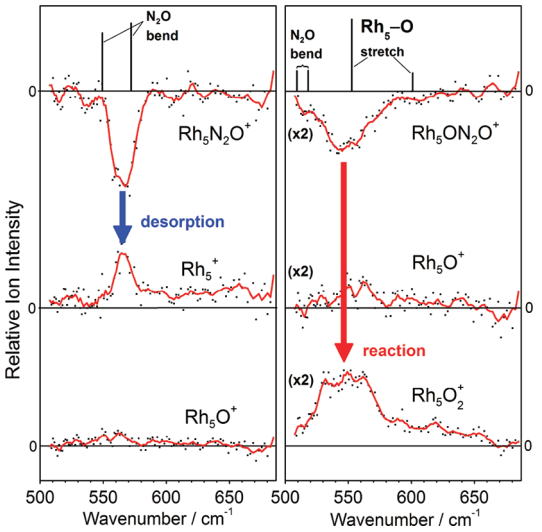

Figure 2. IR-MPD spectra of the $Rh_5N_2O^+$ and $Rh_5ON_2O^+$ complexes in the region of the overlapping N_2O bend and O stretch. Upon IR heating, $Rh_5N_2O^+$ exhibits mainly N_2O desorption resulting in enhancement in the Rh_5^+ signal, whereas the predominant process observed for $Rh_5ON_2O^+$ is surface N_2O decomposition forming the dioxide cluster. The stick spectra represent calculated IR spectra at the DFT level of theory (TPSSh/def2−TZVP).

Here, we report the results of a combined experimental and computational study into the anomalously inert $Rh_5N_2O^+$ complex.

All experiments were performed at the Free Electron Laser for Infrared eXperiments (FELIX) facility in The Netherlands.[19] Rh_n^+ and Rh_nO^+ clusters with molecularly adsorbed nitrous oxide molecules were generated as described previously[17,18] and irradiated by the FELIX infrared beam in the spectral region $20\ \mu m > \lambda > 14.5\ \mu m$ ($500 - 690\ cm^{-1}$), which covers the N_2O bend and O−Rh_n^+ stretch fundamental transitions.

The mid-infrared free electron laser beam counter propagates along the molecular beam, and the two beams temporally overlap before the clusters enter the extraction region of a reflectron time-of-flight mass spectrometer. Mass spectra are collected at a frequency of 10 Hz with the free electron laser enabled every other cycle. IR-MPD spectra are obtained by monitoring the difference in mass spectra recorded with and without the FELIX beam as a function of varying IR photon wavelength. Depletions of parent ion peaks and corresponding enhancements in product peaks serve as a mass spectrometric signal for photon absorption and/or infrared-driven cluster reactivity. All IR spectra are recorded using 0.05 μm wavelength ($\sim$1 cm^{-1}) steps and are averaged over several runs.

The experimental mass spectrum in the region of the Rh_5^+ cluster is shown in Figure 1a. All major mass peaks can be assigned to Rh_5^+ clusters complexed with nitrous oxide ($Rh_5(N_2O)_y^+$), oxygen ($Rh_5O_x^+$), or combinations thereof. Figure 1b shows the effect on the mass spectrum of irradiating the cluster beam in the spectral region of the N_2O bend/O−Rh_n^+ stretch fundamental transitions (which, for Rh_5^+, are spectrally unresolved). In such a difference mass spectrum, a negative signal represents the depletion of particular species upon irradiation. Analogously, a positive peak signifies enhancement of the signal in a particular mass channel resulting from IR-induced fragmentation of a larger mass species. By recording the variation in both parent and daughter ion mass channels as a function of IR wavelength, it is possible to determine the major fragmentation channels for each species.

Both the $Rh_5(N_2O)_y^+$ ($y = 1-3$) and $Rh_5O_x(N_2O)^+$ ($x = 1-3$) signals exhibit large depletion upon irradiation, indicating that these species undergo some form of IR-induced fragmentation. The nature of the processes leading to the loss of these ion signals may be deduced from Figure 1b as well as from the IR spectra recorded simultaneously in all mass channels. Example spectra for species of particular interest are shown in Figure 2. These spectra enable depletions in one mass channel to be compared quantitatively with concomitant enhancements in other channels identifying the fragmentation processes involved. In particular, comparison of the (spectrally integrated) absolute depletions and enhancements in the various spectra provides important information on the branching ratios for various surface processes that ensue. N_2O desorption from larger clusters, e.g., $Rh_5(N_2O)_{n>1}^+$, is observed both as a depletion in the parent $Rh_5(N_2O)_{n>1}^+$ signal and as an enhancement in the $Rh_5(N_2O)^+$ channel but can be accounted for by virtue of the spectral red shift in the $Rh_5(N_2O)_{n>1}^+$ signal.

Consistent with our earlier findings, the depletion in the $Rh_5N_2O^+$ signal is accompanied by a significant enhancement in the bare Rh_5^+ signal, indicating that the predominant process is a simple N_2O desorption (blue solid line, Figure 1b; left-hand side Figure 2). By contrast, only a minimal increase in the Rh_5O^+ signal is observed above the noise level. From the ratio of the integrated enhancements observed in each product channel, we

dx.doi.org/10.1021/jz2012963 |J. Phys. Chem. Lett. 2011, 2, 3053–3057

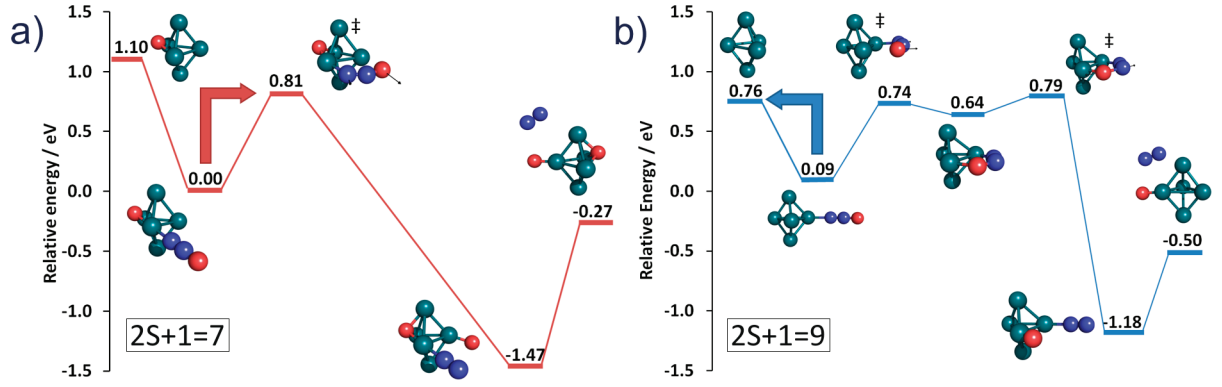

Figure 3. Typical calculated reaction pathways for infrared-induced dissociation of nitrous oxide on TBP motifs of (a) the Rh_5O^+ cluster and (b) the Rh_5^+ cluster. In each case, the starting point is the lowest energy calculated structure for this motif. The energy scales refer to the overall minimum energy structure of each cluster. Note that in the case of $Rh_5(N_2O)^+$ we calculate a SBP structure 0.09 eV lower in energy (see Table 1). A complete set of reaction pathways calculated on all structures calculated to lie within 0.1 eV of the putative global minimum is shown in the SI associated with this article.

estimate that the desorption process accounts for ≥85% of products observed.

These reaction/desorption branching ratios are reversed completely in the case of the $Rh_5ON_2O^+$ complex. In this case, the minimal Rh_5O^+ enhancement indicates the minor role of the N_2O loss channel (blue dashed line, Figure 1b; right-hand side Figure 2). Instead, the dominant enhancement observed is in the dioxide cluster signal, $Rh_5O_2^+$, consistent with a highly efficient cluster surface reaction resulting in N_2O decomposition (solid red line, Figure 1b). This time it is the reactive channel that accounts for ≥85% of the products observed.

In short, a single coadsorbed oxygen atom is enough to transform the fate of the $Rh_5N_2O^+$ cluster when subjected to infrared heating. The results can be summarized as follows:

$$Rh_5(N_2O)^+ + IR \rightarrow \begin{array}{ll} Rh_5^+ + N_2O & \geq 85\% \\ Rh_5O^+ + N_2 & \leq 15\% \end{array}$$

$$Rh_5O(N_2O)^+ + IR \rightarrow \begin{array}{ll} Rh_5O^+ + N_2O & \leq 15\% \\ Rh_5O_2^+ + N_2 & \geq 85\% \end{array}$$

Qualitatively similar enhancements in the reactive channel for the O-adduct species are also observed for other cluster sizes, e.g., $n = 6$. However, these are less pronounced, as the N_2O decomposition channel is already a significant minor channel.

Figure 2 also shows the calculated spectrum in this region at the density functional theory (DFT) level using the TPSSh functional[20] and the def2-TZVP basis set.[21] The spectral splitting in the N_2O bend region of the $Rh_5N_2O^+$ has previously been resolved in cryogenically cooled rare-gas tagging experiments at low IR fluence but is unresolved here.[18] Likewise, in $Rh_5ON_2O^+$ the N_2O bend and O−Rh_n^+ bands are also unresolved. However, for $Rh_6N_2O^+$ and $Rh_6ON_2O^+$, we have shown previously that the surface chemistry exhibits no particular mode-selectivity, with each strongly active IR mode equally efficient in driving the cluster surface decomposition reaction.[18] We therefore expect the surface chemistry to be equally efficient across the merged band in $Rh_5ON_2O^+$.

In an attempt to better understand the effects of the coadsorbed O atom, we have undertaken a detailed computational study of the energetically low-lying structures of the $Rh_5N_2O^+$/$Rh_5ON_2O^+$ clusters and the pathway for reaction. All calculations were carried out using DFT as implemented in the Turbomole v6.1 package.[22,23] As discussed previously,[18] no single exchange−correlation functional is ideal for all of the calculations necessary: low energy structure optimizations, spectral simulations, and reaction pathways. However, the TPSSh[20] meta-hybrid functional provides a good compromise for all three calculations. Triple-ζ valence basis sets (def2-TZVP)[21,24] were used for all atoms, with def2-ecp effective core potentials for the rhodium atoms.

The starting points for the structure calculations were the low energy structures of the bare Rh_n^+ clusters for which experimental evidence exists in the form of recent IR-MPD spectra.[15,16] A wide range of spin states as well as potential oxygen and N_2O binding arrangements was explored, and a table of the low-lying structures of the $Rh_5ON_2O^+$ species identified based on both trigonal bipyramid (TBP) and square-based pyramid (SBP) structures is provided in the Supporting Information (SI) associated with this article. Normal mode analyses confirmed the identity of minima or transition states as well as providing the spectral simulations.

Qualitatively similar surface reaction pathways (N_2O dissociation followed by N_2 loss) to that identified for the $Rh_6N_2O^+$ were found on all low-lying structures of both $Rh_5N_2O^+$ and $Rh_5O(N_2O)^+$ clusters. A complete set of these calculated reaction pathways for structures lying within 0.1 eV of the putative global minimum structure is given in the SI, but a representative example is given in Figure 3. Note that in all cases the final structures are those arrived at using the vector following method. The calculated global minimum structures of these species are given in the SI.

The key factor in determining the branching ratios for reaction versus N_2O desorption is the relative barrier height for the two processes. In order for the surface reaction to compete efficiently with the desorption process, the barrier for the former must lie below the N_2O desorption energy, otherwise the large preexponential (entropic) factor in the effective rate will favor N_2O loss. Table 1 summarizes the calculated values for the N_2O desorption energy and barrier height for the reaction on various low-lying structures. As we have previously reported,[18] we calculate four low-lying isomers of $Rh_5N_2O^+$ to lie within 0.11 eV of the putative global minimum: two based on SBP motifs, two on TBP structures. The far-IR-MPD spectra, however, were inconclusive in identifying which structures we produce in our experiments. Accordingly, we have calculated the reaction pathways for

dx.doi.org/10.1021/jz2012963 |J. Phys. Chem. Lett. 2011, 2, 3053–3057

Table 1. Calculated N_2O Desorption Energies and Surface Reaction Barriers for N_2O Dissociation on Rh_n^+/Rh_nO^+ clusters[a]

	2S + 1	isomer	N_2O desorption energy[b]/eV	reaction barrier[c] /eV	ΔE[d]
$Rh_5N_2O^+$	**9**	**SBP1**	**0.72**	**0.76**	**+0.04**
	9	TBP1	0.73	0.73	+0.00
	9	SBP2	0.68	0.76	+0.08
	9	TBP2	0.67	0.7	+0.03
$Rh_5ON_2O^+$	5	TBP2	1.11	0.77	−0.34
	5	TBP4	1.04	0.72	−0.32
	7	**TBP1**	**1.10**	**0.81**	**−0.29**
	7	TBP3	1.02	0.79	−0.23
$Rh_6N_2O^+$	8		0.68	0.65	−0.03
	10		**0.77**	**0.73**	**−0.04**
$Rh_6ON_2O^+$	8		0.68	0.65	−0.03
	10		**0.77**	**0.70**	**−0.07**

[a] Data for the putative global minimum structure of each species is shown in bold. The reaction pathways and structures for all of the $Rh_5N_2O^+$ and $Rh_5ON_2O^+$ isomers are presented in the SI. $Rh_6N_2O^+$ data are taken from ref 18. [b] $E(Rh_nO_xN_2O^+) - E(Rh_nO_x^+) - E(N_2O)$. [c] $E(TS) - E(Rh_nO_xN_2O^+)$. [d] Reaction Barrier − N_2O desorption energy.

all structures, and the barriers are essentially identical on all (see SI and Table 1).

The calculations provide a clear explanation of the way in which the oxygen atom perturbs the relative branching ratios for N_2O desorption versus dissociation. Figure 3 and Table 1 show that the profound difference in behavior observed for $Rh_5N_2O^+$ and $Rh_5ON_2O^+$ upon IR-heating is not due to any direct involvement of the O-atom in the reaction itself, but rather results from the enhanced binding energy of N_2O to the oxide cluster. As shown in Table 1 (and the pathways in the SI), for all low-lying structures of $Rh_5N_2O^+$, the reaction barrier is at least as high as the N_2O desorption energy ($\Delta E \geq 0$ eV). Hence, the observation that N_2O desorption dominates over dissociation is not surprising, as entropic effects will strongly favor the former. The barrier to surface reaction for the $Rh_5N_2O^+$ is essentially unchanged by the presence of a coadsorbed O-atom. The N_2O binding energy, however, is markedly greater on the Rh_5O^+ cluster (by ca. +0.4 eV) than on Rh_5^+ (see Table 1) taking it above the reaction barrier height ($\Delta E = -0.23$ eV to -0.34 eV depending on the structure). The net effect is that, upon heating, the first channel to open is that for the surface decomposition reaction. In the context of the experiments performed here, this means that significantly fewer (ca. 5−6) IR photons need to be absorbed to reach the top of the reaction barrier than to desorb N_2O. It is important to note that this is true for every pathway calculated on every cluster structure (see SI). Such effects, in which the adsorption of one species influences the binding of another, are not uncommon in small cluster systems, especially noble metal clusters, and can appreciably enhance catalytically important reactions.[10,25]

All calculations in this study were performed under conservation of spin multiplicity. Typically, however, the rhodium oxide clusters (the reaction products) favor a lower spin state than do the putative $Rh_n(N_2O)^+$ or $Rh_nO(N_2O)^+$ global minima. For example, the $Rh_5O_2^+$ ($2S+1 = 5$) state lies marginally (<0.1 eV) lower in energy than the corresponding ($2S + 1 = 7$) state. It thus seems likely that in a real reaction, the $Rh_5ON_2O^+$ (with putative minimum $2S + 1 = 7$, see SI) will undergo a surface crossing during the course of the reaction to the lower electronic surface. Precisely where such a transition might occur is, however, unclear. The additional oxide bond is formed late in the reaction, but our calculations find the transition states on both electronic surfaces to be almost isoenergetic.

In summary, a combined experimental and computational investigation of infrared driven surface dissociation of N_2O on Rh_5O^+ clusters has revealed significant differences to the same process on naked Rh_5^+ clusters with the N_2O decomposition channel strongly promoted on the oxide cluster. Surface reaction accounts for ≥85% of the products observed upon IR heating of $Rh_5O(N_2O)^+$ compared with ≤15% for the same process on $Rh_5(N_2O)^+$. Calculations of the reaction profile indicate that this difference stems from the markedly (0.4 eV) higher N_2O desorption energy on the oxide cluster compared with the naked cluster. As a result, the reactive barrier to N_2O dissociation on $Rh_5ON_2O^+$ lies below the energy required to desorb the nitrous oxide molecule. These findings further illustrate the potential of the infrared driven cluster reactivity technique as a means of probing important surface processes on isolated clusters with size selectivity. The insights provided by comparison of the experimental results with the DFT simulations demonstrate the sensitivity of the method to the topology of the potential energy landscape and in particular the relative barrier heights to different processes.

■ ASSOCIATED CONTENT

Supporting Information. Relative energies and structures of $Rh_5O(N_2O)^+$ based on TBP and SBP motifs. Structure and energy of Rh_5O^+ and $Rh_5O_2^+$ putative global minima. Reaction pathways for the lowest lying $Rh_5O(N_2O)^+$ or $Rh_5(N_2O)^+$ minima. This material is available free of charge via the Internet at http://pubs.acs.org.

■ AUTHOR INFORMATION

Corresponding Author

*(A.F.) Tel: +49 (0)30 8413 5622; fax: +49 (0)30 8413 5603 e-mail: fielicke@fhi-berlin.mpg.de. (S.R.M.) Tel +44(0) 186 527 5156; fax +44(0) 186 527 5410; e-mail: stuart.mackenzie@chem.ox.ac.uk.

Present Addresses

[§]Department of Chemistry, University of Waterloo, Waterloo, Canada.

■ ACKNOWLEDGMENT

We gratefully acknowledge FELIX beamtime provided by Stichting voor Fundamenteel Onderzoek der Materie (FOM) and the skilful assistance of the FELIX staff, particularly Dr. B. Redlich and Dr. A. F. G. van der Meer. We are grateful to Dr. D. M. Rayner for providing the rhodium rod. This work is supported by the Deutsche Forschungsgemeinschaft through research grant FI 893/3-1. W.S.H. is grateful for a Ramsay Memorial Fellowship. D.J.H. thanks the Alexander-von-Humboldt-Stiftung for support. The research leading to these results has received funding from the European Community's Seventh Framework Programme (FP7/2007-2013) under Grant Agreement No. 226716.

REFERENCES

(1) Somorjai, G. A. *Chemistry in Two Dimensions: Surfaces*; Cornell University Press: Ithaca, NY, 1981.

(2) Anderson, M. L.; Ford, M. S.; Derrick, P. J.; Drewello, T.; Woodruff, D. P.; Mackenzie, S. R. Nitric Oxide Decomposition on Small Rhodium Clusters, $Rh_n^{+/-}$. *J. Phys. Chem. A* **2006**, *110*, 10992–11000.

(3) Harding, D.; Ford, M. S.; Walsh, T. R.; Mackenzie, S. R. Dramatic Size Effects and Evidence of Structural Isomers in the Reactions of Rhodium Clusters, $Rh_n^{+/-}$, with Nitrous Oxide. *Phys. Chem. Chem. Phys.* **2007**, *9*, 2130–2136.

(4) Harding, D.; Mackenzie, S. R.; Walsh, T. R. Structural Isomers and Reactivity for Rh_6 and Rh_6^+. *J. Phys. Chem. B* **2006**, *110*, 18272–18277.

(5) Harding, D. J.; Davies, R. D. L.; Mackenzie, S. R.; Walsh, T. R. Oxides of Small Rhodium Clusters: Theoretical Investigation of Experimental Reactivities. *J. Chem. Phys.* **2008**, *129*, 124304.

(6) Torres, M. B.; Aguilera-Granja, F.; Balbas, L. C.; Vega, A. Ab Initio Study of the Adsorption of NO on the Rh_6^+ Cluster. *J. Phys. Chem. A* **2011**, *115*, 8350–8360.

(7) Ford, M. S.; Anderson, M. L.; Barrow, M. P.; Woodruff, D. P.; Drewello, T.; Derrick, P. J.; Mackenzie, S. R. Reactions of Nitric Oxide on Rh_6^+ Clusters: Abundant Chemistry and Evidence of Structural Isomers. *Phys. Chem. Chem. Phys.* **2005**, *7*, 975–980.

(8) Hegedus, L. L.; Mccabe, R. W. Catalyst Poisoning. *Catal. Rev. - Sci. Eng.* **1981**, *23*, 377–476.

(9) Hagen, J.; Socaciu, L. D.; Elijazyfer, M.; Heiz, U.; Bernhardt, T. M.; Wöste, L. Coadsorption of CO and O_2 on Small Free Gold Cluster Anions at Cryogenic Temperatures: Model Complexes for Catalytic CO Oxidation. *Phys. Chem. Chem. Phys.* **2002**, *4*, 1707–1709.

(10) Lang, S. M.; Bernhardt, T. M. Cooperative and Competitive Coadsorption of H_2, O_2, and N_2 on Au_x^+ (x = 3,5). *J. Chem. Phys.* **2009**, *131*, 024310.

(11) Lang, S. M.; Bernhardt, T. M.; Barnett, R. N.; Yoon, B.; Landman, U. Hydrogen-Promoted Oxygen Activation by Free Gold Cluster Cations. *J. Am. Chem. Soc.* **2009**, *131*, 8939–8951.

(12) Lyalin, A.; Taketsugu, T. Cooperative Adsorption of O_2 and C_2H_4 on Small Gold Clusters. *J. Phys. Chem. C* **2009**, *113*, 12930–12934.

(13) Fielicke, A.; von Helden, G.; Meijer, G. Far-Infrared Spectroscopy of Isolated Transition Metal Clusters. *Eur. Phys. J. D* **2005**, *34*, 83–88.

(14) Fielicke, A.; Kirilyuk, A.; Ratsch, C.; Behler, J.; Scheffler, M.; von Helden, G.; Meijer, G. Structure Determination of Isolated Metal Clusters via Far-Infrared Spectroscopy. *Phys. Rev. Lett.* **2004**, *93*, 023401.

(15) Harding, D. J.; Walsh, T. R.; Hamilton, S. M.; Hopkins, W. S.; Mackenzie, S. R.; Gruene, P.; Haertelt, M.; Meijer, G.; Fielicke, A. Communications: The Structure of Rh_8^+ in the Gas Phase. *J. Chem. Phys.* **2010**, *132*, 011101.

(16) Harding, D. J.; Gruene, P.; Haertelt, M.; Meijer, G.; Fielicke, A.; Hamilton, S. M.; Hopkins, W. S.; Mackenzie, S. R.; Neville, S. P.; Walsh, T. R. Probing the Structures of Gas-Phase Rhodium Cluster Cations by Far-Infrared Spectroscopy. *J. Chem. Phys.* **2010**, *133*, 214304.

(17) Hamilton, S. M.; Hopkins, W. S.; Harding, D. J.; Walsh, T. R.; Gruene, P.; Haertelt, M.; Fielicke, A.; Meijer, G.; Mackenzie, S. R. Infrared Induced Reactivity on the Surface of Isolated Size-Selected Clusters: Dissociation of N_2O on Rhodium Clusters. *J. Am. Chem. Soc.* **2010**, *132*, 1448–1449.

(18) Hamilton, S. M.; Hopkins, W. S.; Harding, D. J.; Walsh, T. R.; Haertelt, M.; Kerpal, C.; Gruene, P.; Meijer, G.; Fielicke, A.; Mackenzie, S. R. Infrared-Induced Reactivity of N_2O on Small Gas-Phase Rhodium Clusters. *J. Phys. Chem. A* **2011**, *115*, 2489–2497.

(19) Oepts, D.; van der Meer, A. F. G.; van Amersfoort, P. W. The Free-Electron-Laser User Facility Felix. *Infrared Phys. Technol.* **1995**, *36*, 297–308.

(20) Staroverov, V. N.; Scuseria, G. E.; Tao, J. M.; Perdew, J. P. Comparative Assessment of a New Nonempirical Density Functional: Molecules and Hydrogen-Bonded Complexes. *J. Chem. Phys.* **2003**, *119*, 12129–12137.

(21) Weigend, F.; Ahlrichs, R. Balanced Basis Sets of Split Valence, Triple Zeta Valence and Quadruple Zeta Valence Quality for H to Rn: Design and Assessment of Accuracy. *Phys. Chem. Chem. Phys.* **2005**, *7*, 3297–3305.

(22) Krause, A.; Musso, H.; Boland, W.; Ahlrichs, R.; Gleiter, R.; Boese, R.; Bar, M. All-Cis-1,4,7,10-Cyclododecatetraene - X-Ray Structure-Analysis and Photoelectron-Spectrum. *Angew. Chem., Int. Ed. Engl.* **1989**, *28*, 1379–1381.

(23) Turbomole V6.1 2009, a Development of University of Karlsruhe and Forschungszentrum Karlsruhe Gmbh, 1989−2007, Turbomole Gmbh, since 2007; Available from http://www.turbomole.com.

(24) Weigend, F.; Häser, M.; Patzelt, H.; Ahlrichs, R. RI-MP2: Optimized Auxiliary Basis Sets and Demonstration of Efficiency. *Chem. Phys. Lett.* **1998**, *294*, 143–152.

(25) Bernhardt, T. M. Gas-Phase Kinetics and Catalytic Reactions of Small Silver and Gold Clusters. *Int. J. Mass Spectrom.* **2005**, *243*, 1–29.